A mechanical equivalence for Poisson's ratio and thickness of C-C bonds in single wall carbon nanotubes

2008 J. Phys. D: Appl. Phys. 41 085306

(http://iopscience.iop.org/0022-3727/41/8/085306)

IOP PUBLISHING JOURNAL OF PHYSICS D: APPLIED PHYSICS

J. Phys. D: Appl. Phys. **41** (2008) 085306 (5pp) doi:10.1088/0022-3727/41/8/085306

A mechanical equivalence for Poisson's ratio and thickness of C–C bonds in single wall carbon nanotubes

Fabrizio Scarpa[1,3] **and Sondipon Adhikari**[2]

[1] Department of Aerospace Engineering, University of Bristol, Queens Building, University Walk, BS8 1TR, Bristol, UK

[2] School of Engineering University of Wales Swansea, Swansea SA2 8PP, UK

E-mail: f.scarpa@bris.ac.uk

Received 8 January 2008, in final form 22 February 2008
Published 20 March 2008
Online at stacks.iop.org/JPhysD/41/085306

Abstract

A formulation for the equivalent mechanical properties (Young's modulus, shear modulus and Poisson's ratio) of the C–C bond of CNTs under tensile and bending small deformations is derived. The C–C bonds behave like structural elements with negligible lateral deformation when stretched. The results from the model have been applied to structural mechanics truss assemblies representing single wall nanotube and nanoropes, providing good comparison with existing numerical and experimental results available.

(Some figures in this article are in colour only in the electronic version)

Nano-based materials and structures have seen widespread use in recent times. Typical examples are composites with dispersed nanotubes and nanoparticles [1], and nanoresonators and oscillators for wireless applications [2]. Structural mechanics approaches have been widely considered recently to describe the deformation of carbon nanotubes [3–6, 9]. The basic tenet of this popularity is the possibility of describing the nanotube layout as a frame-like structure, where the primary bonds between atoms are considered equivalent to structural beam elements, and the atoms themselves simulated as lumped masses for vibration simulations [7, 8]. In this way, simulations of mechanical properties at the atomistic level can be performed using classical finite element or matrix structural analysis codes. The elements of structural beam matrices are based on the knowledge of Young's modulus and Poisson's ratio of the beam material when considered isotropic, as well as the inertia properties of the beam section. Li and Chou [4] used the direct equivalence between force constants from total steric potential and mechanical strain energies, therefore avoiding the determination of the equivalent core material properties of the C–C bond. However, they imposed a thickness d (C–C bond diameter) for the tubes of 0.34 nm (interlayer spacing of graphite). This approach has also been taken by To [10], this time considering the shear deformation mechanism of the nanotube to correct the predictions of the mechanical properties. The thickness d of the beam is a parameter on which special focus has been drawn, because it relates to the determination of engineering constants like Young's modulus and equivalent continuum properties of the nanostructures. Different thickness values have been assumed in the open literature, ranging from 0.066 nm from MD simulations [12], to 0.69 nm in equivalent continuum modelling [3]. The scatter of the thickness values originates from the different methods (MD, tight-binding models and DFT analysis, for example), interatomic potentials and specific numerics of the simulations. The so-called 'Yakobson paradox' [13] encapsulates the large scatter of data and contradicting values on Young's modulus SWCNTs. Recently, Huang *et al* have proposed an analytic approach to calculate the tension and bending rigidities of graphene sheets and CNTs using 1st and 2nd generation Brenner potentials, showing that equivalent thickness values depend on the type of mechanical loading and radius of the CNT [14]. Tserpes and Papanikos [5] have used the steric potential–mechanical strain energy equivalence to identify a C–C bond thickness and equivalent Young's and shear modulus of the bond. They identified a thickness d equal to 0.140 nm, having almost the same dimension of the

[3] Author to whom any correspondence should be addressed.

covalent bond length (0.142 nm), Young's modulus E and shear modulus G of 5.59 TPa and 0.871 TPa, respectively. However, the mechanical strain energies expressions used in their approach are related to slender beams, where shear deformation and Poisson's ratio effect of the material are not taken into account. Clearly, for thick beams this assumption is not valid, and an alternative analysis would be required.

A common approach to describe the total steric potential energy of the C–C bonds in a CNT under small linear elastic deformations is the harmonic representation, omitting the electrostatic interaction [3,4]:

$$U_{\text{total}} = U_r + U_\theta + U_\tau. \tag{1}$$

U_r, U_θ and U_τ are, respectively, the energies due to bond stretching, bond angle variation and combined dihedral angle and out-of-plane torsion. Using the harmonic representation, the single energies can be expressed as [4]

$$U_r = \tfrac{1}{2}k_r(\Delta r)^2, \tag{2a}$$

$$U_\theta = \tfrac{1}{2}k_\theta(\Delta\theta)^2, \tag{2b}$$

$$U_\tau = \tfrac{1}{2}k_\tau(\Delta\varphi)^2, \tag{2c}$$

where k_r, k_θ and k_τ are, respectively, the force constants related to bond stretching, bending and torsional stiffness. Bond stretching variation, in-plane and twisting angle increments are indicated by Δr, $\Delta\theta$ and $\Delta\varphi$, respectively. A force model used by some authors in SWCNT mechanical simulations [3,5] is the AMBER one [11]. It must be pointed out that Li and Chou [4] have observed a negligible influence of the force coefficients versus the overall simulated mechanical properties of the carbon nanotubes. In the context of this work, the AMBER force model is chosen for continuity with the models in [3,5]. The AMBER force model constants k_r and k_θ are, respectively, 6.52×10^{-7} N nm^{-1} and 8.76×10^{-10} N nm rad^{-2}, while k_τ is 2.78×10^{-10} N nm^{-1} rad^{-2}. In the structural equivalent mechanics approach, the elastic constants for the equivalent continuum material composing the C–C bonds are determined equating the interatomic interaction energies and the strain energies associated with the mechanical deformation of the structural elements. Assuming that the C–C bonds behave as uniform three-dimensional beams with stretching, torsion and bending capabilities, the strain energies associated with pure axial and torsion loading can be expressed as [4,5]

$$U_{\text{axial}} = \frac{1}{2}K_{\text{axial}}(\Delta L)^2 = \frac{EA}{2L}(\Delta L)^2, \tag{3a}$$

$$U_{\text{torsion}} = \frac{1}{2}K_{\text{torsion}}(\Delta\beta)^2 = \frac{GJ}{2L}(\Delta\beta), \tag{3b}$$

$$U_{\text{bending}} = \frac{1}{2}K_{\text{bending}}(2\alpha)^2 = \frac{EI}{2L}(2\alpha)^2. \tag{3c}$$

In (3*a*) and (3*b*), E and G are the equivalent Young's and shear modulus for the bond, while A and J are the cross-section area and polar moment of inertia. The axial deformation and end beam rotation are expressed by ΔL and $\Delta\beta$. Equation (3*c*) is related to a slender uniform beam with inertia moment I under pure bending, with 2α being the change in rotational angle (bond angle variation) [4].

When using the harmonic potential, equating (2*a*)–(2*b*) and (3*a*)–(3*b*) with the force constants described above and assuming a circular cross-section (CNT thickness) d for the beam, Tserpes and Papanikos [5] found a thickness d equal to 0.140 nm. For deep (thick) beams, shear deformation of the cross-section under bending should be considered, not to overestimate the deflection of the beam [17]. We follow in this case the Tserpes and Papanikos approach to calculate the equivalent continuum thickness of the C–C bond, but considering the shear deformation and the effect of Poisson's ratio of the equivalent continuum material for the covalent bond. The bending spring K_{bending} in equation (3*c*) can be modified therefore as [15]

$$K_{\text{bending}} = EI\frac{4+\Phi}{L(1+\Phi)}, \tag{4}$$

where Φ is the shear deformation constant

$$\Phi = \frac{12EI}{GA_sL^2}, \tag{5}$$

where $A_s = A/F_s$, and F_s being the shear correction factor. Considering the C–C bond as a uniform full constant circular section element, the area and inertia properties of the beam are $A = \pi d^2/4$, $I = \pi d^4/64$ and $J = \pi d^4/32$, where d is the diameter (thickness) of the bond. The shear deflection constant is [16]

$$F_s = \frac{6(1+\nu)}{7+6\nu}, \tag{6}$$

where ν is Poisson's ratio of the beam element material. Imposing the equivalence between Δr and ΔL, as well as between $\Delta\beta$ and $\Delta\theta$, one can obtain the following expressions for Young's and shear modulus from the equivalence between the steric and mechanical strain energies:

$$E = \frac{4k_rL}{\pi d^2}, \tag{7a}$$

$$G = \frac{32k_\theta L}{\pi d^4}. \tag{7b}$$

Inserting expressions (7*a*) and (7*b*) into the definition of shear deformation constant (5) one obtains

$$\Phi = \frac{9\pi^2k_rd^4(1+\nu)}{16L^2\pi^2k_\theta(7+6\nu)}. \tag{8}$$

Imposing the equivalence between the mechanical bending strain energy and U_τ, after substituting (6), (7*a*) and (7*b*) and (8) in (4), one obtains the following implicit relation between d and ν:

$$k_\tau = \frac{\pi k_rd^2(448k_\theta L^2\pi^2+384L^2\pi k_\theta\nu+9k_r\pi^2d^4+9k_r\pi^2d^4\nu)}{16\pi(112k_\theta L^2\pi^2+96L^2\pi^2k_\theta\nu+9k_rd^4\pi^2+9k_rd^4\pi^2\nu)}. \tag{9}$$

Equation (9) has been solved minimizing the norm of the difference between the two sides of the equation using a simplex search method. The value of L used was

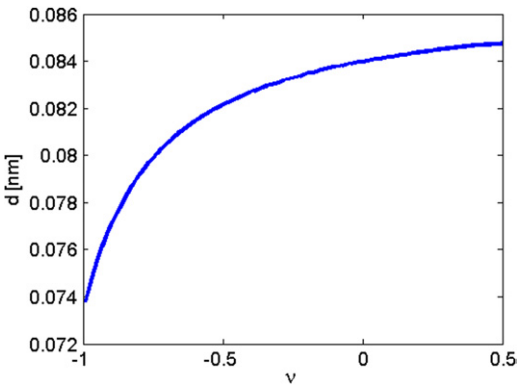

Figure 1. Thickness d over Poisson's ratio of the equivalent C–C bond material from equation (9). $L = 0.142$ nm, $k_r = 6.52 \times 10^{-7}$ N nm^{-1}, $k_\theta = 8.76 \times 10^{-10}$ N nm rad^{-2} and $k_\tau = 2.78 \times 10^{-10}$ N nm^{-1} rad^{-2}.

0.142 nm [3–8]. Poisson's ratio of the equivalent material for the C–C bond has been varied between -1 and 0.5, as per classical homogeneous isotropic and thermodynamically correct materials [17]. The negative Poisson's ratio (NPR) values correspond to auxetic material configurations—the material expands in all directions when pulled in only one [18–20]. Figure 1 shows the relation between Poisson's ratio value ν of the bond and the thickness d satisfying equation (9). A fifth order polynomial interpolation that represents the curve would have coefficients $C_5 = 0.01$, $C_4 = 0.036$, $C_3 = -0.0016$, $C_2 = -0.003$, $C_1 = 0.0025$ and $C_0 = 0.084$ (all dimensions in nm). The admissible values of the thickness range from 0.074 to 0.0848 nm. For the NPR interval, thickness varies between 0.074 and 0.084 nm. It is worth noting the low sensitivity of the C–C bond thickness versus the Poisson's ratio above $\nu = -0.55$. The thickness values are consistent with different results published in the open literature, such as the ones of Zhou *et al* [21] ($d = 0.074$ nm), Tu and Ou-Yang [22] ($d = 0.075$ nm) and Pantano *et al* [23] ($d = 0.075$ nm). Very close to the upper limit of the identified thickness range are the values from Kudin *et al* [24] ($d = 0.089$ nm), and Goupalov [25] ($d = 0.087$ nm). Imposing the isotropic material condition $G = E/2(1+\nu)$ [17] for the equivalent C–C bond medium to constrain equation (9) using a Marquardt algorithm [26], leads to a Poisson's ratio $\nu = 0.034$, and thickness $d = 0.0844$ nm. This marginally positive Poisson's ratio indicates that the C–C bond, when mechanically stretched, has a very low lateral expansion, behaving similarly to cork [23, 27]. The bond Young's modulus E and shear modulus G are 16.71 TPa and 8.08 TPa, respectively. Tserpes and Papanikos [5] calculated values of 5.59 TPa and 0.871 TPa for Young's and shear modulus, for an equivalent Poisson's ratio of 2.15, if the material of the bond is considered isotropic. The above Poisson's ratio value, above the limit of 0.5, could be considered if the equivalent material of the bond is anisotropic [28], or made of solid undergoing non-affine deformations [29].

The Poisson's ratio and thickness values have also been considered as inputs for finite element models of structural truss frames simulating zigzag $(n, 0)$ and armchair (n, n) SWCNTs [4, 5]. Each single covalent bond was represented by a 3D 2-nodes beam with 6° of freedom, shear deformation effects, possessing axial, bending and torsion stiffness capabilities [15]. The CNT models were subjected to pure tensile and bending loading. The tensile Young's modulus Y was determined applying the uniaxial loading F at one end of the tube, and constraining the opposite side. The resulting axial (Δh) deformation was used to calculate the related stiffness, using the relation $Y = (F/A_0)/(\Delta h/h_0)$, where $A_0 = 2\pi Rd$ is the base cross-section area. The tensile CNT models had a maximum fixed length of 6.73 nm. The bending modulus Y_f was obtained applying a central loading F on a bridged–bridged tube (i.e. clamped ends), with an aspect ratio of 20 between the cross-section diameter D and the length of the tube itself. This aspect ratio ensures that the resulting bending modulus can be evaluated with the formula $Y_f = (FL^3/192)/(\delta/I)$ (where δ is the resultant central deflection and I the moment of inertia of the tube), i.e. the tube can be represented by an Euler–Bernoulli beam with no transverse shear effects [17]. For every case, the simulations were carried out using a Newton–Raphson solver, allowing nonlinear geometric deformations. The latter solver option was retained for generality, although the interatomic harmonic potential formulation is valid only for small strains [1, 11]. The total system potential energy $\Pi = U - W$ of the SWCNTs was evaluated for each loading condition, where U is the potential energy of the atoms system and W the virtual work on the loading force. Minimization of the potential energy was carried out with a subproblem zero-order approximation method [30]. Poisson's ratio ν of the C–C bond was constrained between -1 and 0.5, while the thickness d was allowed to vary between 0.06 nm [31] and 0.69 nm [3].

Table 1. Tensile rigidity, thickness and Poisson's ratio for zigzag and armchair tubes. Tube length is 6.73 nm.

R (nm)	ν	d (nm)	E (TPa)	G (TPa)	Yd (GPa nm)	ε_{11}
Zigzag(n,0)						
0.378	0.0344	0.0838	16.79	8.15	205.3	6.12×10^{-4}
0.777	0.0344	0.0839	16.77	8.13	195.8	3.14×10^{-4}
0.935	0.0344	0.0838	16.78	8.14	194.9	2.62×10^{-4}
1.1708	0.0344	0.0838	16.81	8.167	194.4	2.09×10^{-4}
Armchair(n,n)						
0.426	0.0344	0.0826	17.3	8.66	293.9	3.79×10^{-4}
0.585	0.0344	0.0830	17.01	8.46	242.5	3.37×10^{-4}
1.029	0.0344	0.0836	16.88	8.24	198.9	2.33×10^{-4}
1.312	0.0344	0.0836	16.85	8.22	191.1	1.90×10^{-4}

Table 1 shows the values of Poisson's ratios and thicknesses identified for minimum potential energy for zigzag and armchair SWCNT configurations under axial loading. For all CNT configurations, Poisson's ratio related to the minimum potential energy state equal to $0.034 \pm 2\%$, almost identical to the one identified for the above pure isotropic bond condition. The thickness d values were around 0.0838 nm for the different nanotube radii, with 0.7% difference from the pure isotropic case, providing average Young's modulus E of 16.78 TPa and shear modulus G of 8.15 TPa. For all axial loading cases, the maximum axial strain ε_{11} was 6.12×10^{-4}, well within the

Table 2. Bending modulus, thickness and Poisson's ratio for zigzag and armchair SWCNTs. Aspect ratio (tube length/tube diameter) is 20.

Radius (nm)	ν	d (nm)	E (TPa)	G (TPa)	Y_f (TPa)	ε_f
Zigzag						
0.378	0.0344	0.112	16.79	2.54	0.88	3.51×10^{-5}
0.777	0.0344	0.0853	16.77	7.61	1.078	1.84×10^{-5}
0.935	0.0344	0.0842	16.65	8.02	1.079	1.56×10^{-5}
1.1708	0.0344	0.0837	16.81	8.17	1.083	1.24×10^{-5}
Armchair						
0.246	0.0344	0.0773	19.7	11.25	2.7	2.51×10^{-5}
0.585	0.0344	0.0911	14.22	5.85	1.26	1.935×10^{-5}
0.883	0.0344	0.0841	16.65	8.02	1.15	1.54×10^{-5}
1.312	0.0344	0.0836	16.89	8.25	1.075	1.12×10^{-5}

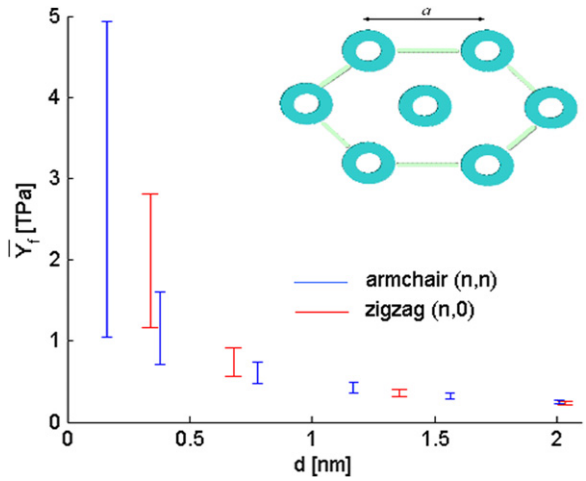

Figure 2. Variation of the bending modulus for SWCNT nanoropes versus tube diameter. $\nu = 0.034$, $d = 0.0844$ nm and $0\,\text{nm} < t_{\text{VdW}} < 0.34\,\text{nm}$.

limits of linear elastic deformation of the tube. The armchair tubes provided a similar behaviour under axial loading, with an average thickness d of 0.0832 nm (1.42% lower than the pure isotropic case), and a Poisson's ratio of $0.034 \pm 2\%$ also in this case. It is interesting to note that the values of the tension rigidity Yd of the carbon nanotubes versus the tube radius R follow the trends of the tension rigidity calculated using the second generation Brenner potential [14], with strong dependence of the stiffness versus chirality and tube radius for $R < 1$ nm. However, the tension rigidity calculated with the Brenner potential predicts a 20% stiffer carbon nanotube compared with the current model. The armchair nanotubes feature higher tension rigidity than the zigzag ones, in agreement with lattice dynamics, tight-binding and analytical models [32].

The bending loading features a different distribution of thickness d compared with the axial loading case, although the equivalent Poisson's ratio ν of the C–C bond remains constant at $0.034 \pm 2.5\%$. From table 2, zigzag tubes have a thickness distribution with decreasing values for increasing radii, with d equal to 0.122 nm for $R = 0.378$ nm. For $R > 1$ nm, the thickness d value stabilizes around 0.0837 nm, 0.8% lower than the pure isotropic case. For armchair configurations, the behaviour of the thickness distribution for $R < 1$ nm is more complex; however, for radii higher than 1 nm the thickness d assumes a similar value to the zigzag configuration. The bending loading simulations have been carried out with maximum bending strains $\varepsilon_f = \delta / L_{\text{tube}}$ of 3.51×10^{-5}. It is worth noting that zigzag and armchair tubes provide different bending modulus Y_f behaviour for smaller radii, the zigzag one increasing for increasing R, the armchair with an inverse relation to the radius. For $R > 1$, both types of tubes tend to provide a flexural Young's modulus of 1.07–1.08 TPa. Wang has observed that for large radii zigzag and armchair configurations tend to provide the same rigidity [33]. Tombler *et al* [34], and Wang *et al* [35] have found experimental values of the flexural modulus of 1.2 TPa for $R < 8$ nm. The initial radii of the nanotubes were computed using the classical geometric definition $R = (\sqrt{3}/2\pi) L \sqrt{m^2 + mn + n^2}$, where m and n are the chiral vector index. However, it must be observed that the formula does not take into account the effect of tube curvature for small radii, while for simple tension loading the CNT radius has little effect [36]. On the overall, however, the values of the flexural modulus calculated with the current model are good in agreement with the experimental findings.

In the open literature, SWCNTs ropes have been tested using AFM methods and the engineering beam theory used to derive the flexural modulus of the nanotube assemblies [37]. A classic packing arrangement for nanotube ropes is the hexagonal one [14, 34, 40] (figure 2). The centre distance l_0 between SWCNTs in the hexagonal packing is $2R + t_{\text{VdW}}$, where t_{VdW} is the distance between CNT walls, depending on van der Walls forces [14]. Using a structural idealization approach to estimate the flexural modulus of the hexagonal cross-section, the bending behaviour of the rope is determined by the axial deformations of the CNTs and the transport moment effect that they provide to the centre of gravity of the section [38].

Each CNT has a polar moment of inertia I_c equal to

$$I_c = \frac{\pi}{4}\left[\left(R + \frac{d}{2}\right)^4 - \left(R - \frac{d}{2}\right)^4\right]. \tag{10}$$

The moment of inertia I_{hex} of a hexagonal packing of tubes with area A_c and moment of inertia I_c with respect to the horizontal axis at a distance l_0 is

$$I_{\text{hex}} = 4\left(I_c + \left(3\frac{l_0^2}{2}\right)^2 A_c\right) + 3I_c. \tag{11}$$

Considering only the axial stiffness contribution from the CNTs under bending of the whole nanorope section, the flexural modulus of the nanobundle can be expressed as

$$\bar{Y}_f = Y \frac{I_{\text{hex}}}{I_h}, \tag{12}$$

where $I_h = (11\sqrt{3}/4)(2T + t_{\text{VdW}})^4$ is the inertia moment of the solid hexagonal section. Equation (12) can therefore be

explicated as

$$\bar{Y}_f = Y\left[\frac{20\sqrt{3}\pi R^3 d}{3(2R+t_{\mathrm{VdW}})^4} + \frac{7\sqrt{3}\pi R d^3}{33(2R+t_{\mathrm{VdW}})^4} + \frac{64\sqrt{3}\pi R^2 t_{\mathrm{VdW}} d}{11(2R+t_{\mathrm{VdW}})^4} + \frac{16\sqrt{3}\pi R t_{\mathrm{VdW}}^2 d}{11(2R+t_{\mathrm{VdW}})^4}\right]. \quad (13)$$

Figure 2 shows the variation of the rope flexural modulus for armchair and zigzag nanotubes, when $t_{\mathrm{VdW}} = 0$ (neglecting van der Walls forces) and $t_{\mathrm{VdW}} = 0.341$ nm (equilibrium distance between two graphene planes [14]). The simulations have been carried out for $\nu = 0.034$ and $d = 0.0844$ nm. The higher the CNT radius, the lower the sensitivity of the van der Walls forces on the overall flexural modulus of the rope. For $R > 0.4$ nm, $\bar{Y}_f$ assumes values ranging from 1.15 ± 0.45 TPa, to 0.42 ± 0.1 TPa, in line with the 1 TPa measurements by Salvetat *et al* [37] and Krishnan *et al* [39] (0.9–1.7 TPa).

In summary, when considering an equivalent continuum truss approach to describe the mechanical properties of CNTs, in order to use correctly the harmonic potential for the equivalent mechanical properties of the C–C bond, the shear deformation and equivalent Poisson's ratio of the equivalent bond material should be considered when inputting values for Young's and shear modulus of the truss element. From deep beam theory and minimization of the potential energy of the nanotube during axial and flexural loading, the C–C bond assumes a Poisson's ratio of 0.034, showing therefore negligible lateral deformation when stretched. The thickness of the bond assumes a value close to 0.084 nm, with slight variation under linear elastic loading for axial and bending mechanical charges. The structural mechanics models with Poisson's ratio shear correction for the C–C bonds provide similar results to existing models and experimental values in the literature, both tensile modulus, bending modulus of SWCNTs and bending loading of nanoropes.

Acknowledgment

The authors wish to thank the referees for their constructive comments.

References

[1] Lakhtakia A (ed) 2004 *Nanometer Structures* (Bellingham, WA: SPIE Press)
[2] Li C and Chou T W 2003 *Phys. Rev.* B **68** 073405
[3] Odegard G M, Gates T S, Nicholson L M and Wyse K E 2002 *Compos. Sci. Technol.* **62** 1869–80
[4] Li C and Chou T W 2003 *Int. J. Solids Struct.* **40** 2487
[5] Tserpes K I and Papanikos P 2005 *Composites* B **36** 468
[6] Li C and Chou T W 2004 *Phys. Rev.* B **69** 073401
[7] Li C and Chou T W 2004 *Appl. Phys. Lett.* **84** 123
[8] Li C and Chou T W 2003 *Phys. Rev.* B **68** 073405
[9] Wu Y, Zhang X, Leung A Y T and Zhong W 2006 *Thin-Walled Struct.* **44** 667
[10] To C W 2006 *Finite Elem. Anal. Des.* **42** 404
[11] Cornell W D *et al* 1995 *J. Am. Chem. Soc.* **117** 5179
[12] Yacobson B I, Brabec C J and Bernholc J 1996 *Phys. Rev. Lett.* **76** 2511
[13] Shenderova O A, Zhirnov V V and Brenner D W 2002 *Crit. Rev. Solid State Mater. Sci.* **27** 227
[14] Huang Y, Wu J and Wang K C 2006 *Phys. Rev.* B **74** 245413
[15] Przemieniecki J S 1968 *Theory of Matrix Structural Analysis* (New York: McGraw-Hill)
[16] Young W C and Budynas R G 2002 *Roark's Formulas for Stress and Strain* 7th edn (New York: McGraw-Hill)
[17] Timoshenko S and Goodier J N 1951 *Theory of Elasticity* (New York: McGraw-Hill)
[18] Lakes R S 1987 *Science* **235** 1038
[19] Evans K E, Nkansah M A, Hutchinson I J and Rogers S C 1991 *Nature* **353** 124
[20] Scarpa F, Blain S, Lew T, Perrott D, Ruzzene M and Yates J R 2007 *Composites* A **38** 280
[21] Zhou X, Zhou J and Ou-Yang Z C 2000 *Phys. Rev.* B **62** 13692
[22] Tu Z C and Ou-Yang Z C 2002 *Phys. Rev.* B **65** 233407
[23] Pantano A, Parks D M and Boyce M C 2004 *J. Mech. Phys. Solids* **52** 789
[24] Kudin K N, Scuseria G E and Yakobson B I 2001 *Phys. Rev.* B **64** 235406
[25] Goupalov S V 2005 *Phys. Rev.* B **71** 085420
[26] Marquardt D 1963 *SIAM J. Appl. Math.* **11** 431
[27] Gibson L J, Easterling K E and Ashby M F 1981 *Proc. R. Soc. Lond.* A **377** 99
[28] Ting T C T and Cheng T 2005 *Q. J. Mech. Appl. Math.* **58** 73
[29] Lakes R 1991 *J. Mater. Sci.* **26** 2287
[30] Denn M M 1969 *Optimization by Variational Methods* (New York: McGraw-Hill)
[31] Vodenitcharova T and Zhang L C 2003 *Phys. Rev.* B **68** 165401
[32] Chang T, Geng J and Guo X 2005 *Appl. Phys. Lett.* **87** 251929
[33] Wang Q 2004 *Int. J. Solid Struct.* **41** 5451
[34] Tombler T W, Zhou C, Kong J, Dai H, Liu L, Jayanthi C S, Tang M and Wu S Y 2000 *Nature* **405** 769
[35] Wang Z L, Gao R P, Poncharal P, De Heer W A, Dai Z R and Pan Z W 2001 *Mater. Sci. Eng.* C **16** 3
[36] Jiang H, Zhang P, Liu B, Huang Y, Geubelle P H, Gao H and Wang K C 2003 *Comput. Mater. Sci.* **28** 429
[37] Salvetat J P, Briggs G A D, Bonard J M, Bacsa R R, Kulik A J, Stockli T, Burnham T and Forro L 1999 *Phys. Rev. Lett.* **82** 944
[38] Megson T H G *Aircraft Structures for Engineering Students* 3rd edn (London: Arnold)
[39] Krishnan A, Dujardin E, Ebbesen T W, Yianilos P N and Treacy M M J 1998 *Phys. Rev.* B **58** 14013
[40] Liu Z and Qin L C 2005 *Carbon* **43** 2146